ISSN 0029-3865

CNPq

CBPF- CENTRO BRASILEIRO DE PESQUISAS FÍSICAS

Notas de Física

CBPF-NF-020/93

Coercive Field and Domain Wall Properties in $(Dy_xY_{1-x})Fe_2$ and $(Er_xY_{1-x})Fe_2$ Intermetallic Compounds

by

K.M.B. Alves, L.C. Sampaio, A.P. Guimarães and S.F. da Cunha

Rio de Janeiro
1993

ISSN 0029-3865

CBPF-NF-020/93

Coercive Field and Domain Wall Properties in $(Dy_xY_{1-x})Fe_2$ and $(Er_xY_{1-x})Fe_2$ Intermetallic Compounds†

by

K.M.B. Alves, L.C. Sampaio, A.P. Guimarães and S.F. da Cunha*

Centro Brasileiro de Pesquisas Físicas — CBPF/CNPq
Rua Dr. Xavier Sigaud, 150
22290-180 Rio de Janeiro – RJ, Brasil

* Permanent address:
Departamento de Física e Química
Universidade Federal do Espírito Santo – UFES
29069 – Vitória, ES – Brasil

† To be published in J. Magn. Magn. Mat.

Abstract

Isothermal DC magnetization measurements were performed in $(R_x, Y_{1-x})Fe_2$ (with $R = Dy$ and Er, in the range of $0 < x < 1$, for several temperatures. The observed pronounced decay of the coercive field H_c with temperature was fitted with an exponential. The coercive field H_c and the propagation field H_p show a maximum value in the range of 30-40% concentration for Dy or Er. At low temperatures, the coercive field H_c decreases exponentially with temperature, near 50% R concentration. These results can be explained by intrisinc domain wall pinning. Time relaxations of the remanent magnetization are measured and attributed to domain wall surface deformations.

Introduction

Many intermetallic compounds, Laves phase, AB_2 type, present domain wall pinning. In particular, high anisotropy energies present in some compounds give rise to an intrinsic coercive field due to very narrow domain walls. This behaviour has been observed in many pseudo-binaries compounds, in particular in those where the magnetic moment of the A elements couples anti parallel to Fe moments in B sites. Examples are the $R(Fe_{1-x}Al_x)_2$ compounds with $R = Dy$, Tb, Er and Hf [1-5].

In a previous paper [6] we have reported that magnetic measurements in $(R_xY_{1-x})Fe_2$ for $R = Tb$, Ho, and Dy showed that Dy has a much larger propagation field, comparatively to other rare-earths.

In the present work we study the behaviour of magnetic properties, such as coercive fields H_c, propagation fields H_p, variation with temperature and time effects of the remanent magnetization for some concentrations of $R = Dy$ and Er in $(R_xY_{1-x})Fe_2$, in the range $0 \leq x \leq 1$.

Experimental

The polycrystalline $(R_xY_{1-x})Fe_2$ samples were prepared in an arc-melting furnace under a purified argon atmosphere, in stoichiometric proportions of high purity metals. Heat treatment at 900 $^\circ C$ for 100 hours in an argon atmosphere was perfomed, followed by X-ray analysis of powdered samples at room temperature, which showed a single phase with C15 crystal structure.

The magnetization measurements were made in a PAR vibrating sample magnetometer. The samples were zero field cooled and the measurements above 4.2 K were made by increasing continuously the temperature.

Results

We have performed measurements of hysteresis loops after zero field cooling (ZFC) at several temperatures, with applied fields of up to 12.5 kOe for the compounds with $R = Dy$ and Er. Differences between ZFC and FC (field cooling) hysteresis loops were not detected. These loops are shown in fig. 1

for $R = Dy$ and in fig. 2 for Er. We observe that the coercive fields depend on temperature for both Dy and Er. The curves of coercive field H_c obtained in the ZFC regime, versus temperature, for some concentrations of R are shown in fig. 3 for Dy, and fig. 4 for Er. The continuous line is an exponential fit from the low temperature points.

In the demagnetizing region of the hysteresis loop a time dependence of the magnetization was detected. ZFC measurements of magnetization as a function of time for several fields near the coercive field at some temperatures, for 20% Dy, were made. For each temperature, we have taken the curve with the lowest starting magnetization (different in each case) and plotted in fig. 5. Since these correspond to different points on the hysteresis loops, the curves do not follow a temperature sequence.

Discussion

In the ZFC hysteresis loops there appears a propagation field H_p in the initial curve, defined as the field beyond which the domain walls can move. Its value decreases with increasing temperature; H_p was determined from the initial magnetization curves. The systems $(R,Y)Fe_2$ (for $R = Dy$ or Er), present maxima in the curves of propagation field H_p as a function of concentration. For a concentration of 30% R, values of about 8 kOe of H_p for $R = Dy$ and 3 kOe for $R = Er$ are observed at 4.2 K (see fig. 6). In a recent paper [6], we have associated the observed reduction in the spin echo intensities in NMR measurements to an increase in H_p, i.e., to a blocking of domain walls for fields $< H_p$.

The same behaviour as a function of concentration was observed for the coercive field H_c (fig. 7). In the demagnetization region of the hysteresis loop, a time effect was observed which is ascribed to the appearance of deformations in the domain wall. Therefore the field value given for the coercive field is that value necessary to cancel the magnetization in the hysteresis loop measured with a rate of 54 Oe/s under a maximum field of 12.5kOe.

The variation of H_p and H_c with concentration as shown in figs. 6-7, was expected, usually corresponding to a maximum inhomogeneity of exchange and anisotropy energies near the iso-concentration range, metallurgical effects, etc. But another phenomenon can contribute to explain these maxima.

It is known [7] that systems of compounds $(R_xY_{1-x})Fe_2$ for $R=Dy$, Gd, Tb and Er present compensation points in the temperature dependence of the magnetization in a certain range of concentration. As shown by Piercy and Taylor [8], for $R=Dy$, equilibrium points (where the magnetizations of the two sub-lattices cancel each other), appear near 30-40% Dy and also, the maximum of H_c occurs at about 35% Dy, at 4.2K. Our results for the dependence of H_c with Dy concentration agree with those of Piercy and Taylor.

The most interesting feature is the strong temperature dependence of the coercive field, which, as follows, is interpreted in terms of wall pinning. In figures 3 and 4 the temperature dependence of H_c is fitted with an exponential function. This behaviour is related to the decrease of the domain wall pinning and is important for the magnetization process at low temperatures.

It is known that systems with high anisotropy have narrow domain walls (since $\delta \propto (J/K)^{1/2}$, where δ is the wall width, and J and K are the exchange and anisotropy constants, respectively). Van den Brock and Zijlstra [9] have shown that the domain wall energy is different if its center coincides with an atomic plane or if it is located between two planes; this energy difference ΔV gives rise to an intrinsic coercive field $H_c \propto \Delta V/D$ (D is the interplanar distance). Hilzinger and Kronmüller [10] showed that the intrinsic coercivity due to intrinsic domain wall pinning is larger for narrow walls, through the relationship $H_c \propto \Delta V \propto exp[-\pi(\delta/D)]$. On the other hand, impurities and defects are responsible for another kind of domain wall pinning, i.e., the extrinsic pinning, and consequently for the extrinsic coercive field. As these intrinsic and extrinsic wall pinnings are independent, the coercive field can be written as a sum of both contributions [11]:

$$H_c(T) = H_{c,intr}(T) + H_{c,extr}(T) \qquad (1)$$

In figs. 3 and 4 the two contributions can be detected. As we approach the intermediate concentrations (where H_c values are larger), we observe that an exponential decay of H_c indicates (according to [10]) that the intrinsic domain wall pinning dominates at low temperatures.

To study the observed time effects, measurements are made by stopping the hysteresis loop at a field near the coercive field and detecting the time variation of the magnetization. The results obtained with this procedure for some temperatures in the compound with 20% Dy are shown in fig. 5. The curves can be fitted with $M(t) = M_{T_0} - ct\ ln\ t$ where M_{T_0} is a different

constant for each temperature; the plot of dM/dt vs $1/H$ for these data gives straight lines that converge to H_o [12] only at low temperatures. Therefore, we could not draw any conclusions on the activation energies. This time relaxation may be related to deformations of the wall surface (kink creation) by a thermal activation process [13].

In conclusion, at low temperature, the intrinsic domain wall pinning takes place for $R = Dy$ and Er in the $(R_xY_{1-x})Fe_2$ system, which is caused by high anisotropy and narrow domain walls.

Acknowledgements

The authors acknowledge the collaboration of H.J. dos Santos for carrying out some magnetic measurements.

Captions

1. $(Dy_xY_{1-x})Fe_2$ hysteresis loops at different temperatures for 20% Dy, 30% Dy and 40% Dy.

2. $(Er_xY_{1-x})Fe_2$ hysteresis loops at different temperatures for 20% Er and 30% Er.

3. Temperature dependence of the coercive field H_c for $R = Dy$ in $(Dy_xY_{1-x})Fe_2$ for different concentrations.

4. Temperature dependence of the coercive field H_c in $(Er_xY_{1-x})Fe_2$ for 20% Er and 30% Er.

5. Time dependence of the remanent magnetization for $(Dy_xY_{1-x})Fe_2$, at different temperatures.

6. Concentration dependence of the propagation field H_p for $R=Dy$ and Er in $(R_xY_{1-x})Fe_2$ at 4.2K.

7. Concentration dependence of the coercive field H_c for $R=Dy$ and Er in $(R_xY_{1-x})Fe_2$ at 4.2K.

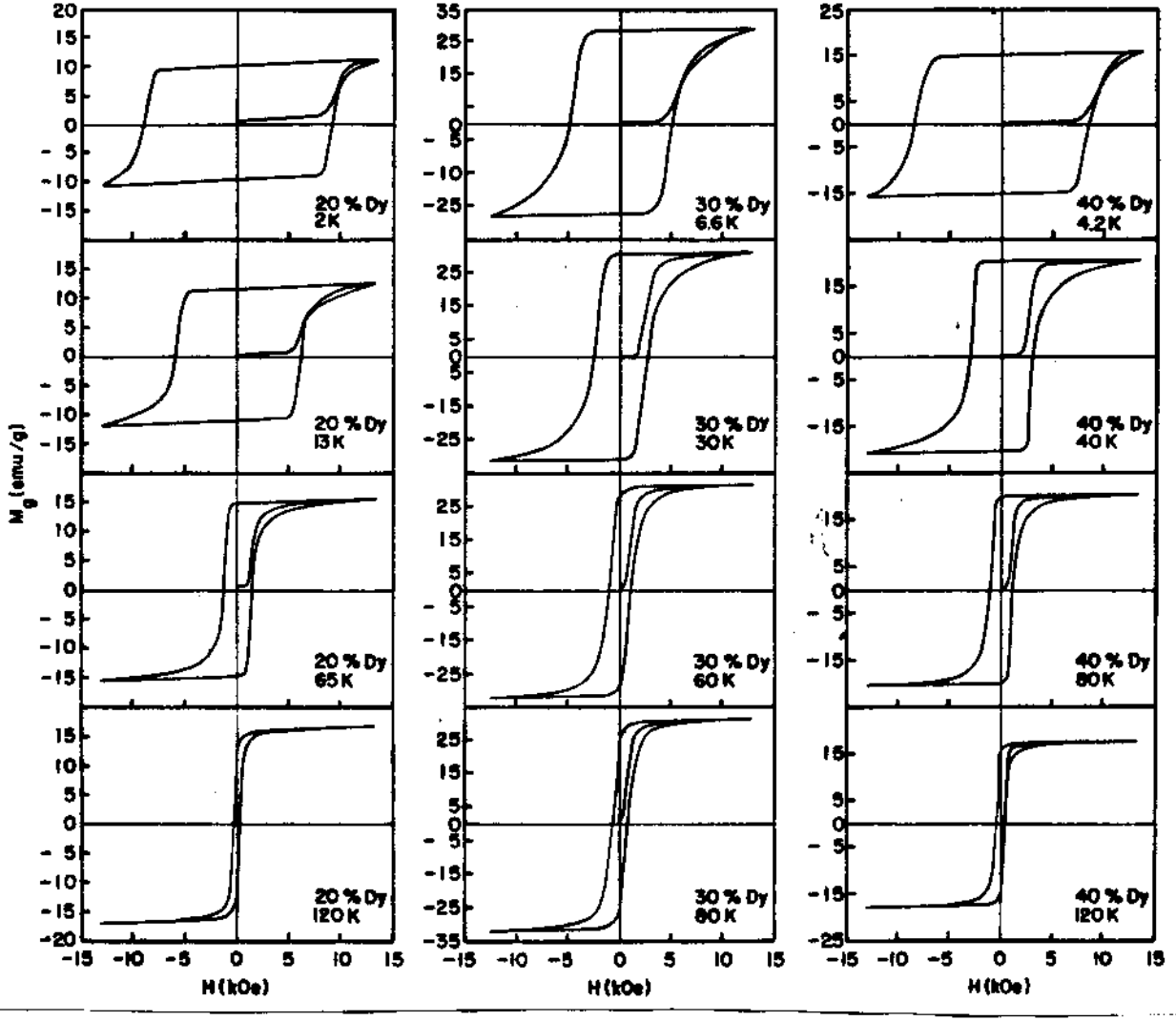
20 % Dy
2K
20 % Dy
13K
20 % Dy
65K
20 % Dy
120K
30 % Dy
6.6K
30 % Dy
30K
30 % Dy
60K
30 % Dy
80K
40 % Dy
4.2K
40 % Dy
40K
40 % Dy
80K
40 % Dy
120K
M_g (emu/g)
H(kOe)
H(kOe)
H(kOe)

FIG. 1

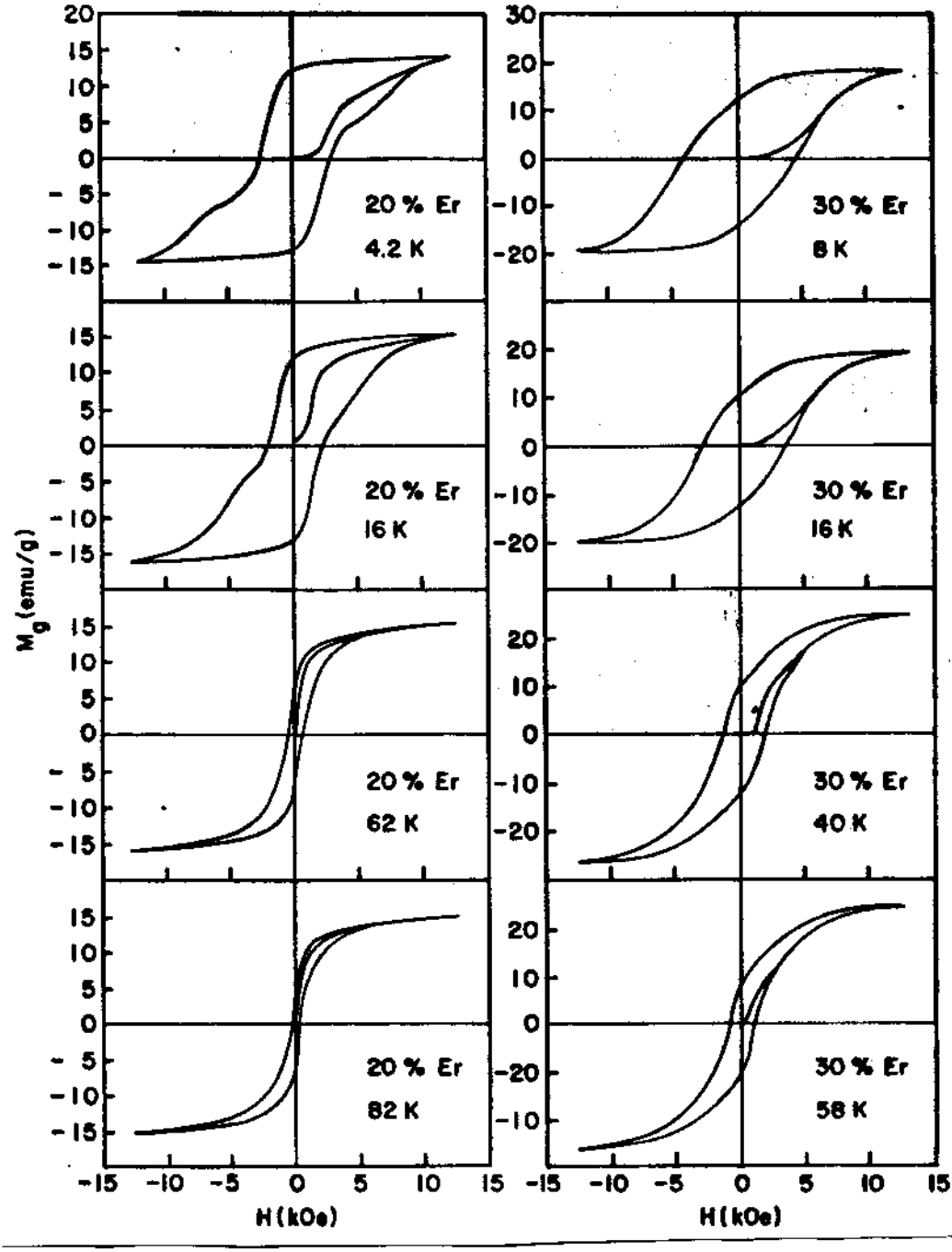
20 % Er
4.2 K
30 % Er
8 K
20 % Er
16 K
30 % Er
16 K
20 % Er
62 K
30 % Er
40 K
20 % Er
82 K
30 % Er
58 K
M_g (emu/g)
H(kOe)
H(kOe)

FIG. 2

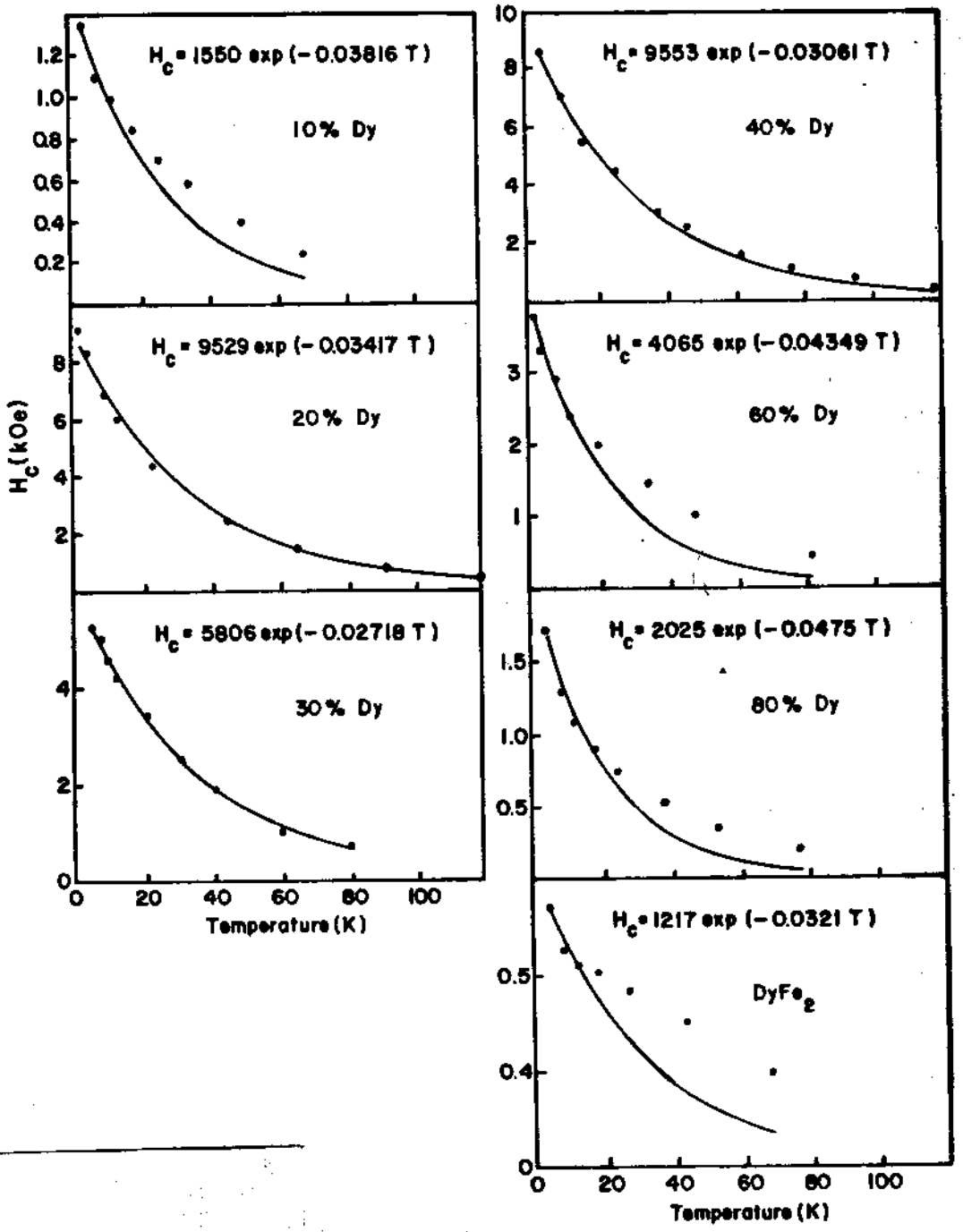
$H_c = 1550 \exp(-0.03816\ T)$
10% Dy
$H_c = 9553 \exp(-0.03061\ T)$
40% Dy
$H_c = 9529 \exp(-0.03417\ T)$
20% Dy
$H_c = 4065 \exp(-0.04349\ T)$
60% Dy
$H_c = 5806 \exp(-0.02718\ T)$
30% Dy
$H_c = 2025 \exp(-0.0475\ T)$
80% Dy
$H_c = 1217 \exp(-0.0321\ T)$
$DyFe_2$
H_c(kOe)
Temperature (K)
Temperature (K)

FIG. 3

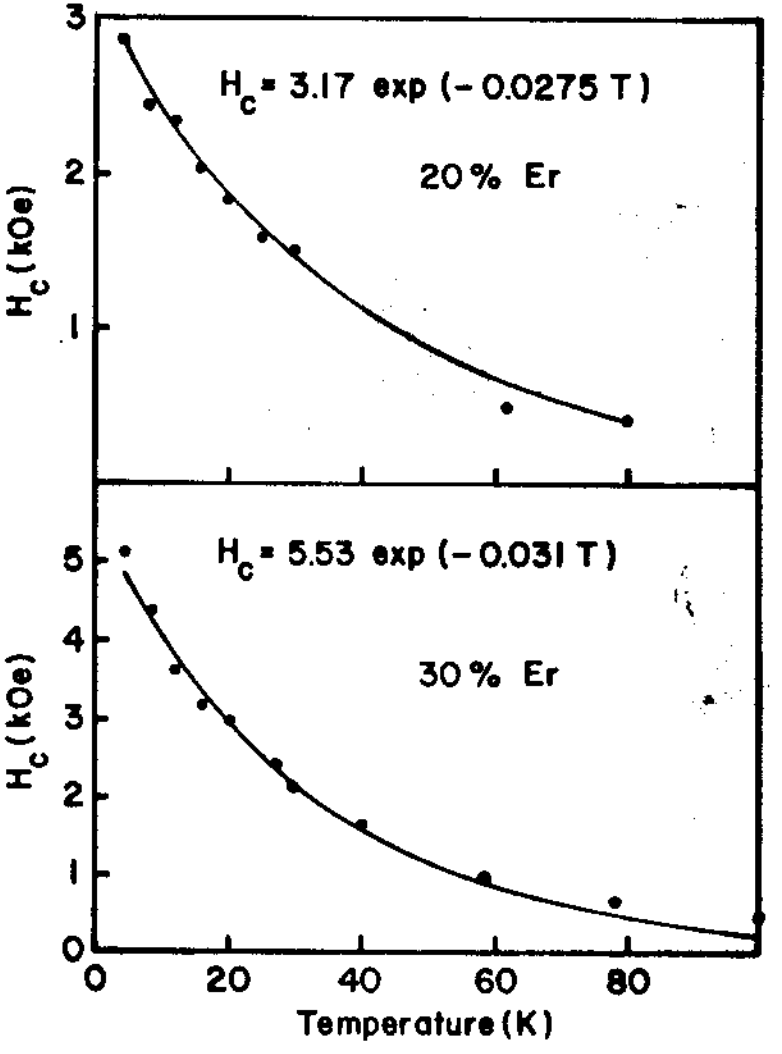
$H_c = 3.17 \exp(-0.0275\,T)$
20% Er
$H_c = 5.53 \exp(-0.031\,T)$
30% Er
H_c (kOe)
H_c (kOe)
Temperature (K)
0
20
40
60
80
1
2
3
4
5

FIG. 4

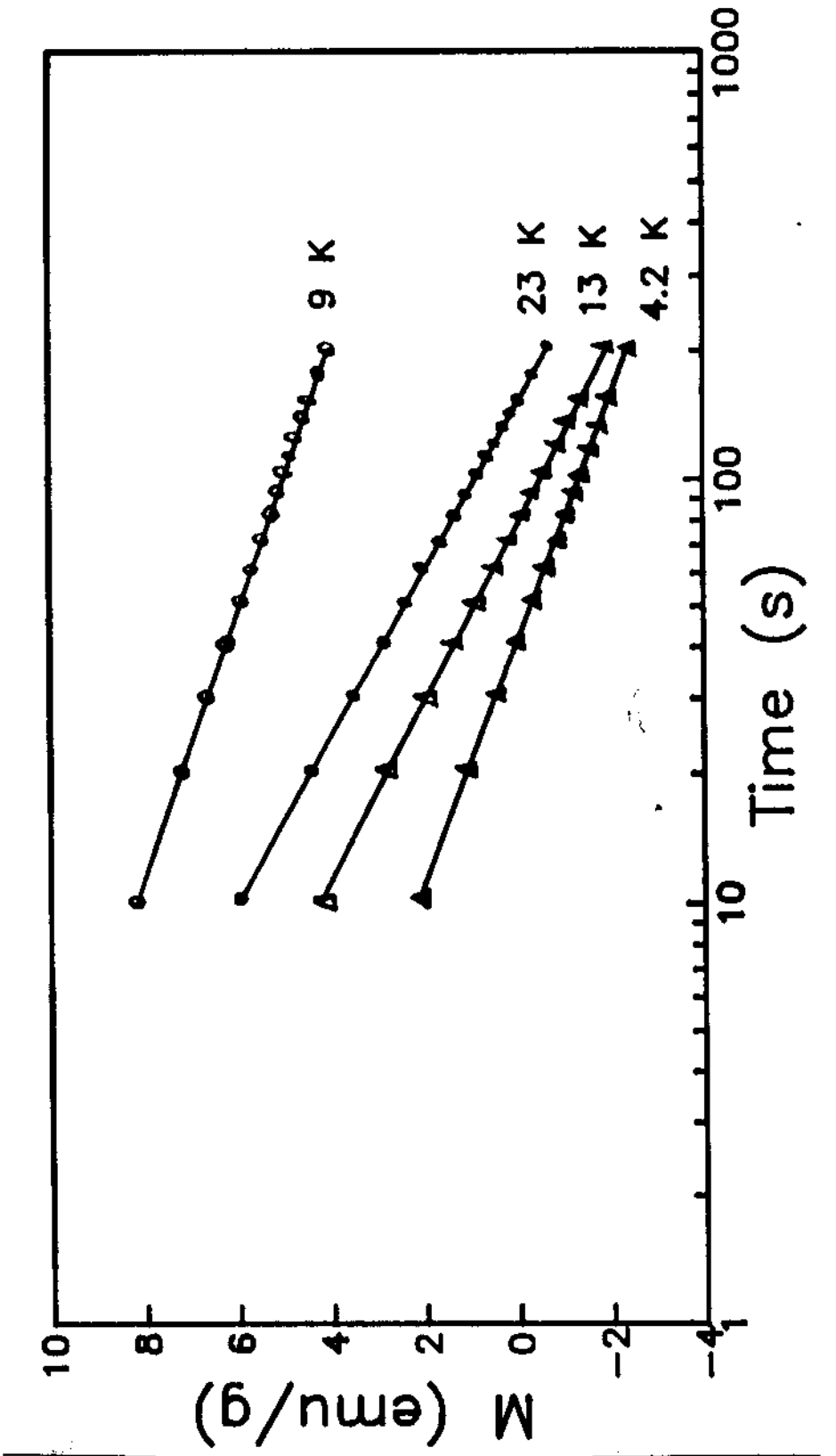

FIG. 5

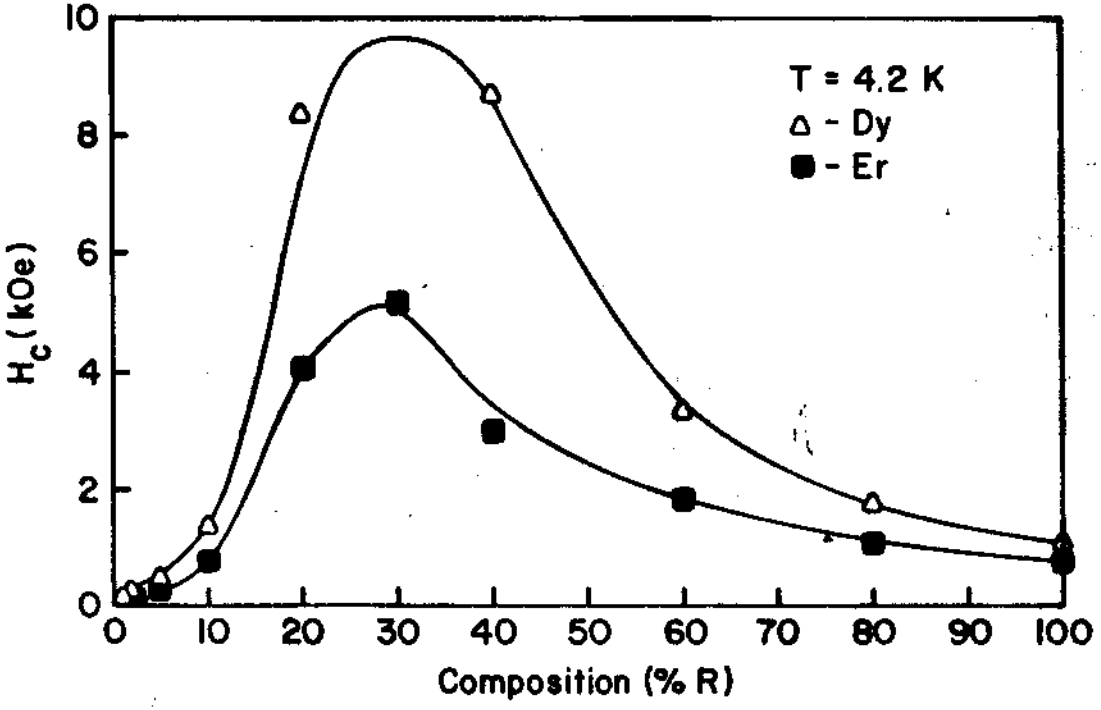
T = 4.2 K
Δ - Dy
■ - Er
H_c (kOe)
Composition (% R)
0
2
4
6
8
10
0
10
20
30
40
50
60
70
80
90
100

FIG. 6

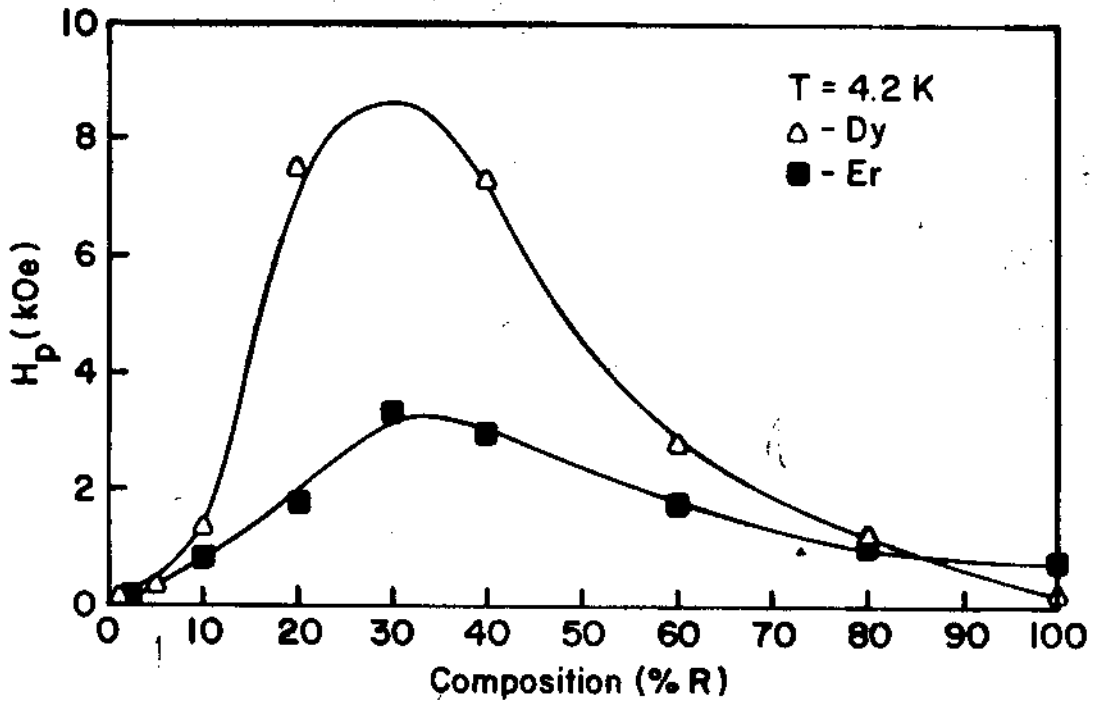
T = 4.2 K
Δ - Dy
■ - Er
H_p (kOe)
Composition (% R)
0
2
4
6
8
10
0
10
20
30
40
50
60
70
80
90
100

FIG. 7

References

[1] W.D. Zong, J. Lan and Z.X. Liu, J. Magn. Magn. Mat. 68 (1987) 197.

[2] W.D. Zong, J. Lan and G.Z. Li., J. Magn. Magn. Mat. 74 (1988) 39.

[3] V. Sima, R. Grössinger, V. Sechovsky and H. Sassik, J. Phys. F 14 (1984) 981.

[4] H. Osterreicher, J. Appl. Phys. 42 (1971) 5137; 34 (1973) 1267.

[5] L.C. Sampaio and S.F. da Cunha, J. Magn. Magn. Mat. 99 (1991) 145.

[6] K.M.B. Alves, N. Alves, L.C. Sampaio, S.F. da Cunha and A.P. Guimarães, J. Appl. Phys. 67 (9) (1990) 5867.

[7] K.H.J. Buschow and R.P. van Stapele, J. Appl. Phys. 41 (10) (1970) 4066.

[8] A.R. Piercy and K.N.R. Taylor, J. Appl. Phys. 39 (2) (1968) 1096.

[9] J.J. van den Brock and H. Zijlstra, IEEE Trans. Mag. MAG-7 (1971) 226.

[10] H.R. Hilzinger and H. Kronmüller, Phys. Stat. Sol. (b) 54 (1972) 593; (b) 59 (1973) 71.

[11] R. Kütterer, H.R. Hilzinger and H. Kronmüller, J. Magn. Magn. Mat. 4 (1977) 1.

[12] B. Barbara and M. Uehara, Physica 86-88B (1977) 1481.

[13] T. Egami, Phys. Stat. Sol. (a) 19 (1973) 747.